Cancer Letters 442 (2019) 464–474

Contents lists available at ScienceDirect

Cancer Letters

journal homepage: www.elsevier.com/locate/canlet

Original Articles

Ovarian cancer cell-derived lysophosphatidic acid induces glycolytic shift and cancer-associated fibroblast-phenotype in normal and peritumoral fibroblasts

Rangasudhagar Radhakrishnan[a], Ji Hee Ha[a,b], Muralidharan Jayaraman[a,b], Jinsong Liu[c], Katherine M. Moxley[a,d], Ciro Isidoro[e], Anil K. Sood[f], Yong Sang Song[g], Danny N. Dhanasekaran[a,b,*]

[a] Stephenson Cancer Center, The University of Oklahoma Health Sciences Center, Oklahoma City, OK, 73104, USA
[b] Department of Cell Biology, The University of Oklahoma Health Sciences Center, USA
[c] Department of Pathology, The University of Texas M. D. Anderson Cancer Center, Houston, TX, 77030, USA
[d] Department of Obstetrics & Gynecology, The University of Oklahoma Health Sciences Center, Oklahoma City, OK, 73104, USA
[e] Department of Health Sciences, Università del Piemonte Orientale, Novara, Italy
[f] Department of Gynecologic Oncology & Reproductive Medicine, and the Center for RNA Interference and Non-Coding RNA, The University of Texas MD Anderson Cancer Center, Houston, TX, 77030, USA
[g] Cancer Research Institute, Seoul National University, College of Medicine, Seoul, 151-921, South Korea

ARTICLE INFO

Keywords:
Ovarian-cancer
Cancer-associated fibroblasts
Lysophosphatidic acid
Hypoxia-inducible factor 1
HIF1
Glycolysis

ABSTRACT

Cancer-associated fibroblasts (CAFs) play a critical role in cancer progression, metastasis, and therapy resistance. Molecular events that confer CAF-phenotype to predecessor-cells are not fully understood. We demonstrate here that the ovarian cancer cell-conditioned medium (OCC-CM) induces CAF-phenotype in MRC5 lung-fibroblasts and it can be mimicked by LPA. While OCC-CM and LPA stimulated the expression of cellular CAF-markers by 3-days, they induced aerobic glycolysis, a metabolic marker for CAF, by 6 hrs. OCC-CM/LPA-induced glycolysis in lung (MRC5) as well as ovarian fibroblasts (NOF151) was inhibited by the LPA-receptor antagonist, Ki16425. Ovarian cancer patient-derived ascitic fluid-induced aerobic glycolysis in both NFs and Ovarian CAFs and it was inhibited by Ki16425. Further analysis indicated that LPA upregulated HIF1α-levels and the silencing of HIF1α attenuated LPA-induced glycolysis in both NOFs and CAFs. These results establish LPA-induced glycolytic-shift as the earliest, potentially priming event, in NF to CAF-transition. These findings also identify a role for LPA-LPAR-HIF1α signaling-hub in the maintenance of the glycolytic-phenotype in CAFs. Our results provide evidence that targeted inhibition of LPA-mediated metabolic reprogramming in CAFs may represent an adjuvant therapy in ovarian cancer.

1. Introduction

Cancer-associated fibroblasts (CAFs), which form the major constituent of the tumor stroma, play an important role in tumor progression, metastasis, and therapy resistance [1–6]. CAFs are highly heterogeneous population of cells with diverse cellular origins [7]. Cancer cells recruit and induce transformation of the tumor resident endothelial cells, epithelial cells, mesenchymal or hematopoietic stem cells, smooth muscle-cells, and quiescent normal fibroblasts (NFs) to CAFs through paracrine signaling mechanisms [1,4–8]. Despite the progenitor role of multiple cell types in the origin of CAFs, the primary route for their origin appears to be the activation of the resident fibroblasts by cancer cells [9]. Irrespective of the cellular origin, CAFs collectively provide an optimal growth niche for the accelerated cancer growth, cancer-angiogenesis, and invasive metastasis through autocrine as well as paracrine signaling pathways [4,10–12]. With the observation that the bidirectional communications between cancer cells and CAFs play a major role in therapy resistance and disease prognosis in

Abbreviations: αSMA, α-smooth muscle actin; NF, normal fibroblast; NOF, normal ovarian fibroblast; CAF, cancer associated fibroblast; ECAR, extracellular acidification rate; FAP, fibroblast activating protein; HIF1α, Hypoxia-inducible Factor 1α; LPA, Lysophosphatidic Acid; LPAR, LPA Receptor; OCC-CM, ovarian cancer cell-conditioned medium; TME, Tumor microenvironment

* Corresponding author. Stephenson Cancer Center, The University of Oklahoma Health Sciences Center, Oklahoma City, OK, 73104, USA.
E-mail address: danny-dhanasekaran@ouhsc.edu (D.N. Dhanasekaran).

https://doi.org/10.1016/j.canlet.2018.11.023
Received 17 September 2018; Received in revised form 16 November 2018; Accepted 21 November 2018

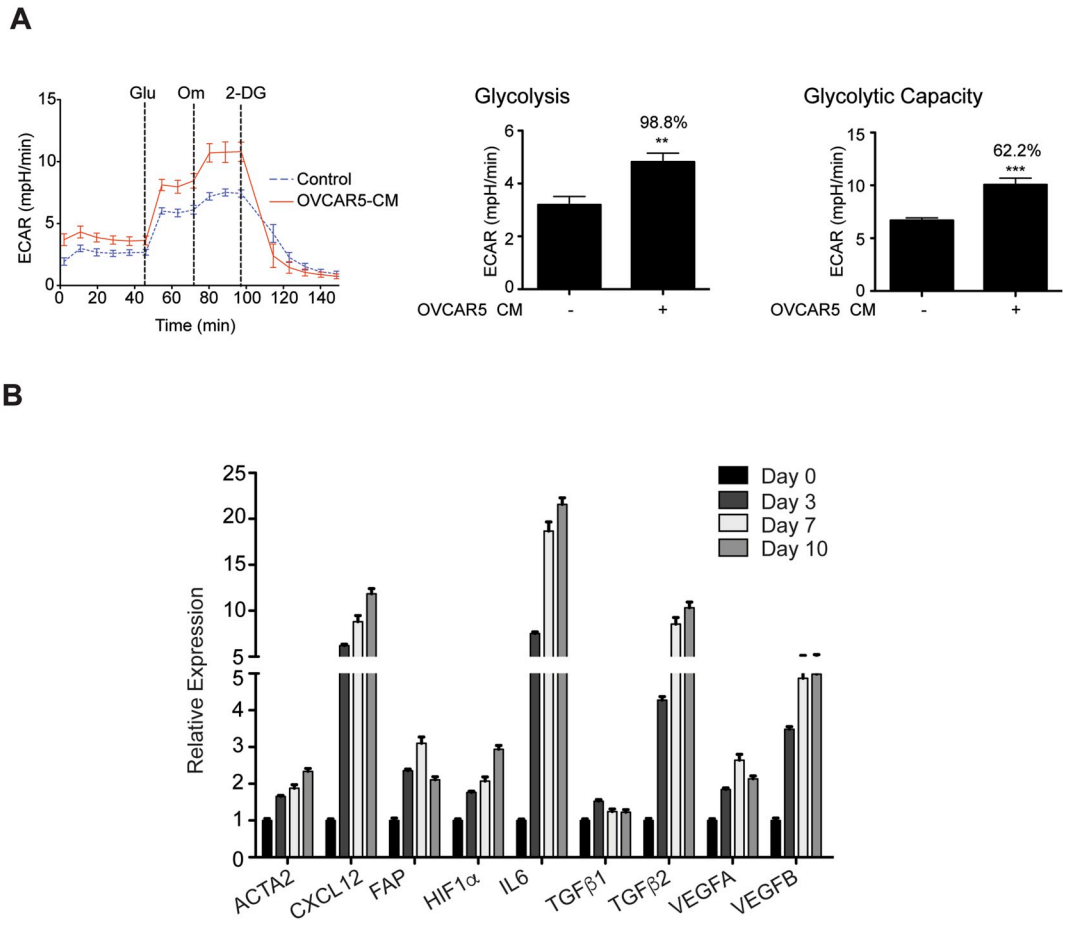

Fig. 1. Ovarian Cancer Cell-conditioned Medium induces CAF-phenotype in MRC5 lung fibroblasts. A. Serum-starved MRC5 fibroblasts cells were stimulated with OVCAR5-CM (40%) continuously for 5 days and ECAR was determined over time using XFe96 extracellular flux analyzer. ECAR was measured every 8 min (Left Panel). Glucose (10 mM), oligomycin (1 μM) and 2-DG (50 mM) were added at the indicated time-points. Rate of glycolysis and glycolytic capacity derived from the ECAR analysis with OVCAR5-CM stimulation are presented as bar charts. Each experiment was repeated at least three times and the results are from a representative analysis. Error bars indicate SEM (n = 4 to 8 parallel determinations). Percentile change over the basal level is denoted over the bars of the chart. Statistical significance between OCC-CM treated and untreated cells was determined by Student's *t*-test (*P < 0.05, **P < 0.005, ***P < 0.0005). **B.** Serum-starved MRC5 fibroblasts were stimulated with OVCAR5-CM as above continuously for 10 days, the cells were collected at the indicated time points, and RT-qPCR analysis was carried out for the above CAF markers by following the standard protocol. Fold changes over control values are presented. The experimente was repeated thrice and the results are from a representative experiment.

many cancers, there has been great interest to define the mechanism through which cancer cells activates the cells in the tumor microenvironment (TME), especially the quiescent fibroblasts to CAFs, so that a therapeutic strategy for co-targeting cancer cells and CAFs can be developed [13–15].

CAFs differ from their normal counterparts by the acquisition of distinct functional and physicochemical phenotypic changes. These include the expression of myofibroblast-specific markers FAP and αSMA, growth factors TGFβ1, TGFβ2, PDGF, PDGFRα, PDGFRβ, βFGF, and periostin, neo-vascularization marker VEGF, chemokine/cytokines IL6 and CXCL12, extracellular matrix proteins such as tenascin-C and neuron glial antigen-2, and structural proteins vimentin, desmin, and fibroblast specific protein-1 [16–21]. While none of these markers are unique to CAFs, a combination of these markers has been often used to identify CAFs. However, a major and key functional feature that distinguishes CAFs from their normal counterparts is their acquired metabolic reprogramming towards aerobic glycolysis [22,23]. Glycolysis in CAFs leads to the synthesis and secretion of lactate and pyruvate that are taken up by the cancer cells to sustain their growing anabolic needs [23–25]. However, the mechanism by which cancer cells induce the functional differentiation of NFs into CAFs with glycolytic phenotype is far from clear [7,8,26]. This is especially true in the case of ovarian cancers, which is the leading cause of death among gynecological malignancies [27].

Recently, we have shown that Lysophosphatidic acid (LPA), synthesized by the ovarian cancer, stimulates aerobic glycolysis in cancer cells by eliciting a pseudohypoxia-adaptive response through a signaling nexus involving Gαi2, Rac1, NOX1, ROS, and HIF1α [28]. Taken together with the observation that cancer cell derived ROS and the resultant accumulation of HIF1α trigger glycolytic shift in CAFs [29,30], we hypothesized that the ovarian cancer cell derived LPA could induce the functional differentiation of normal fibroblasts (NOFs) into CAFs through a similar mechanism involving HIF1α. To test, we investigated the role of LPA present in ovarian cancer cell-conditioned medium (OCC-CM) as well as ovarian cancer patient-derived ascitic fluid in inducing functional differentiation of normal lung and ovarian fibroblasts to CAF-phenotype by monitoring their glycolytic rate in a metabolic flux analyzer. We also tested whether LPA is involved in maintaining the glycolytic phenotype of fully differentiated ovarian CAFs. Our results indicate that LPA stimulates glycolysis in both the normal and cancer-associated fibroblasts along with the expression of CAF-specific phenotypic markers. We also demonstrate that the ascitic fluid-induced glycolytic shift can be inhibited by Ki16425, an LPA-receptor antagonist, thus establishing LPA-LPAR paracrine signaling in ovarian cancer context. In addition, we demonstrate that the glycolysis stimulated by LPA is abrogated by silencing the expression of HIF1α.

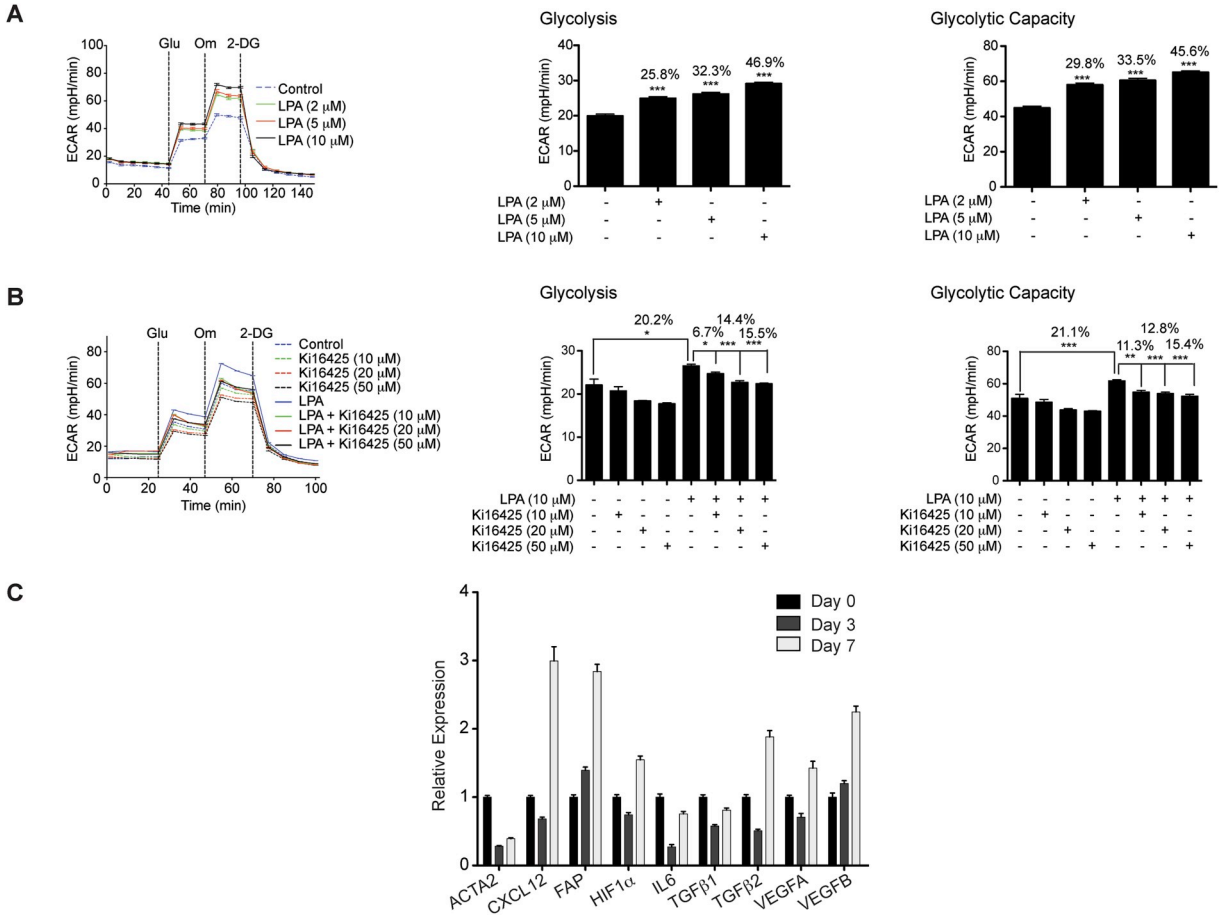

Fig. 2. LPA induces CAF-phenotype in MRC5 lung fibroblasts. A. MRC5 fibroblasts were serum starved overnight and stimulated for 6 h with 2, 5, or 10 μM LPA. ECAR was determined every 8 min. ECAR profile over time (Left Panel), glycolytic rate and glycolytic capacity (Right Panel) from a representative analysis is presented. Mean and SEM (n = 10 to 12 parallel determinations) is shown. Percentile change over the basal level is denoted over the bars of the chart. Statistical significance was determined by Student's *t*-test (*P < 0.05, **P < 0.005, ***P < 0.0005). **B.** MRC5 cells were pre-treated with different dose of LPA inhibitor Ki16425 (10, 20 and 50 μM) 1 h prior to 10 μM LPA treatment for 6h. Change in ECAR was analyzed using XFe96 analyzer and glycolysis and glycolytic capacity data from a representative analysis is presented. Mean and SEM (n = 3 to 4). Percentile change over the basal level is denoted over the bars of the chart. Statistical significance was determined by Student's *t*-test (*P < 0.05, **P < 0.005, ***P < 0.0005). **C.** MRC5 fibroblasts were stimulated with LPA continuously for 7 days, the cells were collected at the indicated time points, and quantitative RT-qPCR analysis was carried out for the indicated CAF markers. Fold changes over control values are presented above the respective bar diagram. The graph above is a representative experiment from three different repeats.

Our studies presented here identify a driving role for LPA-LPAR signaling in inducing aerobic glycolysis and thus a critical priming event in NOF to CAF differentiation. In addition, we demonstrate that this signaling loop can be inhibited by LPA-antagonist or HIF1α-siRNA in both NOFs and CAFs, thereby identifying it as a signaling locus for targeting both the induction and maintenance of CAF-phenotype.

2. Materials and methods

2.1. Cell lines, reagents, and culture methods

Human lung fibroblast MRC5 and OVCAR5 cells were grown and maintained in Dulbecco's modified Eagle's medium (DMEM) (Mediatech, Manassas, VA) whereas immortalized normal ovarian fibroblast (NOF151) and ovarian cancer associated fibroblasts (CAF147, CAF148) were grown and maintained in MCDB:M199 medium supplemented with EGF (10 ng/ml) following the previously published methods [31]. All the above growth media were supplemented with 10% FBS (Gemini Bio-Products, West Sacramento, CA), penicillin-streptomycin 5000 U/mL (Mediatech, Manassas, VA) at 37 °C in a 5% CO_2 incubator. These media containing 0.2% BSA (Cat # BP9704-100; Fisher Scientific, Pittsburg, PA). 18.1 Lysophosphatidic acid (Cat # 250091 1-oleoyl-2-hydroxy-sn-glycero-3-phosphate) was obtained from Avanti Polar Lipids (Alabaster, AL) and dissolved into 10 mM stock solutions in PBS with 0.1% BSA and stored at −80 °C until use. LPA-receptor antagonist Ki16425 (Cat # 5056) was procured from Tocris Bioscience (Minneapolis, MN). The siGENOME non-targeting siRNA (Cat # D-001206-13-05) and siGENOME SMARTpool HIF1α siRNAs (Cat # M-004018-05-0005) were obtained from Dharmacon (Lafayette, CO).

2.2. Collection of ovarian cancer cell-conditioned medium (CM)

Ovarian cancer cell-conditioned-medium was collected following our previously published methods [32]. Cells growing in growth medium were replaced with respective serum starvation medium containing 0.2% BSA and 1% Penicillin-Streptomycin. After 48 h, the medium was collected centrifuged at 600g for 20 min to remove cellular debris and filtered using a 0.22 μM filter and stored in −80 °C for use in ovarian fibroblasts. In experiments requiring the transfection of siRNAs, cells were transfected with non-targeting siRNA or with HIF1α -targeting siRNA (100 nM) using a Nucleofector II system from Lonza (Allendale, NJ) using manufacturer's protocol for fibroblasts (Program # U-023). Cells were collected at 48 h after transfection and used for further analysis.

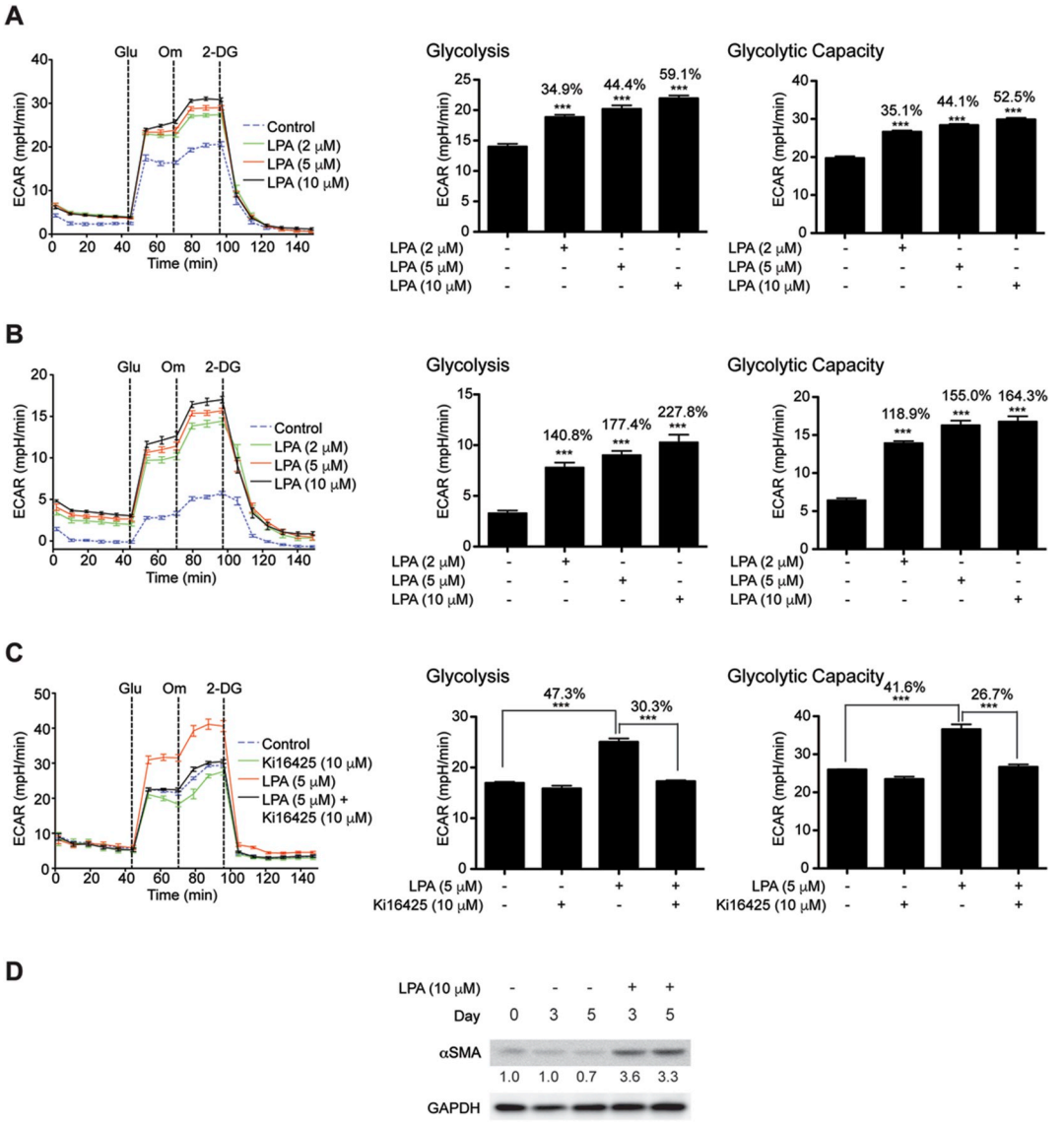

Fig. 3. LPA induces CAF-phenotype in NOFs. A & B. NOF151 cells were serum starved overnight and stimulated for 6 h with 2, 5, or 10 μM LPA (Panel A) or 48 h (Panel B). ECAR was determined every 8 min. ECAR profile over time (Left Panel), glycolytic rate and glycolytic capacity (Right Panel) from a representative analysis is presented. Mean and SEM (n = 9 to 12 parallel determinations) is shown. Percentile change over the basal level is denoted over the bars of the chart. Statistical significance was determined by Student's *t*-test (*P < 0.05, **P < 0.005, ***P < 0.0005). **C.** NOF151 cells were pre-treated with 10 μM of LPA inhibitor Ki16425 1 h prior to stimulation with LPA for 6 h. Change in ECAR was analyzed using XFe96 analyzer and glycolysis and glycolytic capacity data from a representative analysis is presented. Percentile inhibition over the control level is denoted over the bars of the chart. Mean and SEM (n = 6 to 9 parallel determinations). **D.** NOF151 cells were stimulated with 10 μM LPA for the indicated time point and cells were collected and immunoblot analysis was carried out for the CAF marker αSMA. The blot was stripped and probed for GAPDH to be used as loading control. Protein bands were quantified and fold changes over the control value (0-day) is presented below the αSMA-bands.

2.3. Ovarian cancer patient-derived ascitic fluid

Patient-derived ascitic fluid was processed from the ascites samples of patients at the Stephenson Cancer Center, University of Oklahoma Health Science Center, Oklahoma City, Oklahoma. The study was approved by the OUHSC Office of Human Research Participant Protection (HRPP) Institutional Review Board and samples were collected with the informed consent from the patients. Ascitic fluid samples were collected following previously published methods [33]. Cell-free ascitic fluid was prepared as follows: 50 ml of Ascites from patients were centrifuged at 600g for 5 min in room temperature. The supernatant was carefully transferred and used for further analysis.

2.4. Determination of LPA concentration

The concentration of LPA in OCC-CM and ovarian cancer patient-derived ascitic fluid were quantified by ELISA using a commercially available LPA assay kit (Echelon Biosciences, Salt Lake City, UT; Cat #: K-2800S) following manufacturer's protocol. The assay plates were read at the wavelength of 450 nm and the concentrations of LPA in culture medium and ascitic fluid samples were quantified from a standard curve, constructed with the known concentration of LPA.

2.5. Seahorse XFe96 extracellular flux analysis

The extracellular acidification rate (ECAR) was determined in Seahorse XFe96 Extracellular Flux analyzer (Agilent, Billerica, MA) using the XF Glycolysis Stress Kit, following the manufacturer's

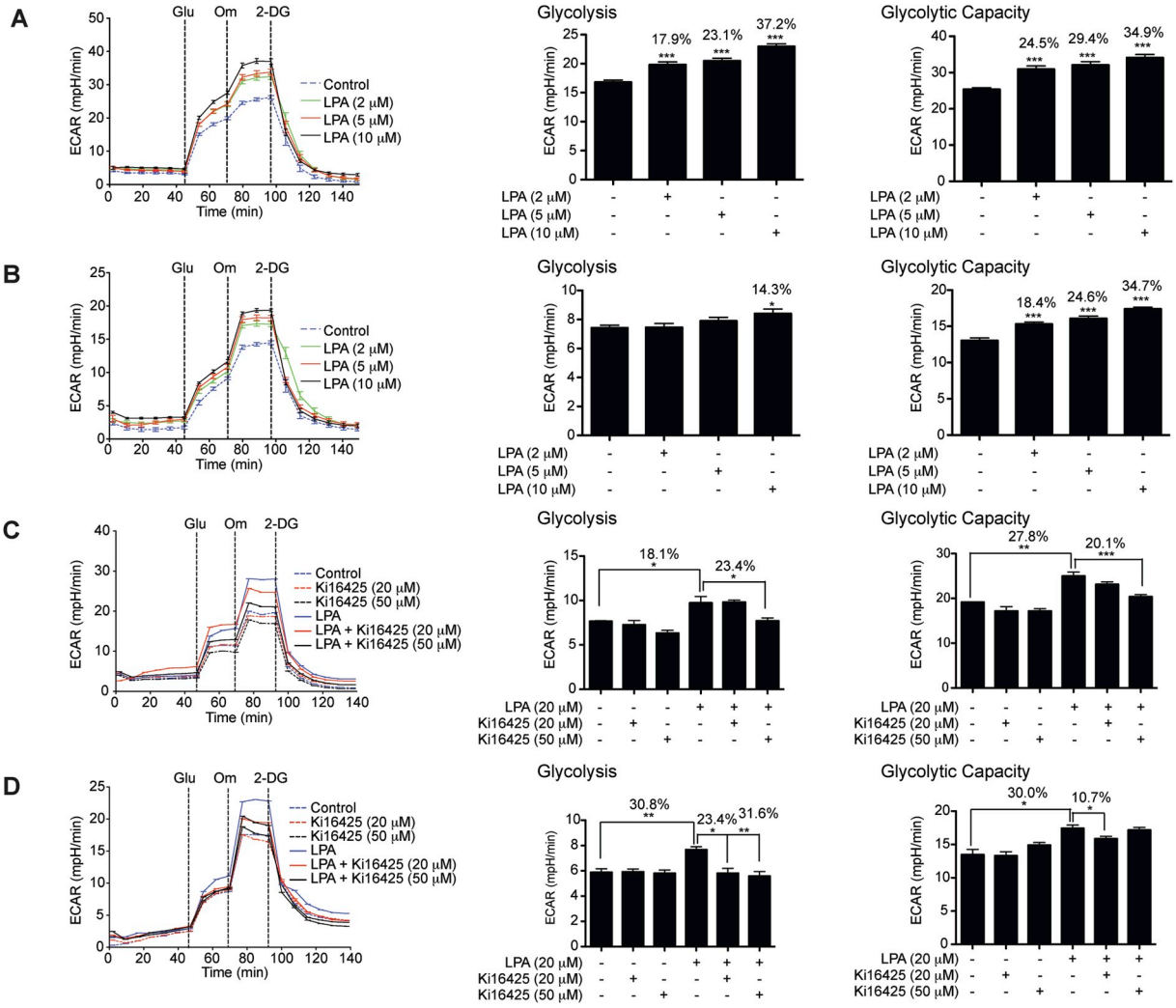

Fig. 4. LPA induces glycolysis in differentiated ovarian CAFs. A & B. Ovarian Cancer associated fibroblasts CAF147 (*Panel A*) and CAF148 (*Panel B*) cells were serum starved overnight and stimulated with 2, 5, and 10 μM LPA for 6 h. Extracellular flux analysis was carried out. ECAR profile over time (Left Panel), glycolytic rate and glycolytic capacity (Right Panel) from a representative analysis is presented. Mean and SEM (n = 11 to 12 parallel determinations) is shown. Percentile change over the basal level is denoted over the bars of the chart. **C & D.** CAF147 and CAF148 cells were pre-treated with Ki16425 (20 and 50 μM) for 1 h and then 10 μM LPA was added to the medium. After 6 h of LPA-stimulation, ECAR analysis was carried out. Data presented are ECAR changes over time (*Left panels*) and glycolysis and glycolytic capacity (Right Panels). Percentile inhibition over the control level is denoted over the bars of the chart. Mean and SEM (n = 3 to 6 parallel determinations). Statistical significance was determined by Student's *t*-test (*P < 0.05, **P < 0.005, ***P < 0.0005).

instructions and our previously published methods [28]. Initial analyses were carried out with cell numbers ranging from 1×10^4 cells/well to 6×10^4 cells/well with 1×10^4 cells increments and observed that there were no cell number dependent changes in the experimental results. Results using 2×10^4 cells/well are presented. The data was analyzed and exported using the Seahorse Wave software (Agilent, Billerica, MA) to the GraphPad Prism (La Jolla, CA) to obtain the graphs and bar charts and also carry out statistical analyses.

2.6. Immunoblot analysis

Immunoblot analysis was carried out according to our previously published methods [32] and developed with a Kodak Image Station 4000 MM. The bands were quantified using ImageJ software (http://rsb.info.nih.gov/ij/). Antibodies to αSMA (Cat # ab7817) were obtained from Abcam (Cambridge MA). HIF1α antibody (Cat # 610959) was procured from BD Transduction labs (San Jose, CA). Antibodies to GAPDH (Cat # CB1001) and β-Actin (Cat # 8457L) were procured from Calbiochem (Burlington, MA) and Cell Signaling Technologies (Danvers, MA) respectively.

2.7. Quantitative real time PCR analysis

Total RNA was extracted from fibroblasts using Qiagen RNeasy Plus kit (Qiagen, Valencia, CA) by following the manufacturer's instructions. cDNA synthesis was carried out using iScript cDNA synthesis kit (Bio-Rad, Carlsbad, CA). Real-time quantitative PCR (RT-qPCR) was carried out using the cDNA from the above step using SsoAdvanced SYBR green PCR kit (Bio-Rad, Carlsbad, CA) in a Bio-Rad CFX96 Real time PCR Detection System. Primers used in the RT-qPCR analyses were provided in the supplementary data (Table S1). The data were normalized to the values obtained with the house-keeping genes GAPDH and GusB. Results were expressed as fold change over the control values.

2.8. Statistical analysis

All statistical analysis was performed using GraphPad Prism (La Jolla, CA) by two-tailed student's *t*-test with Welch's correction.

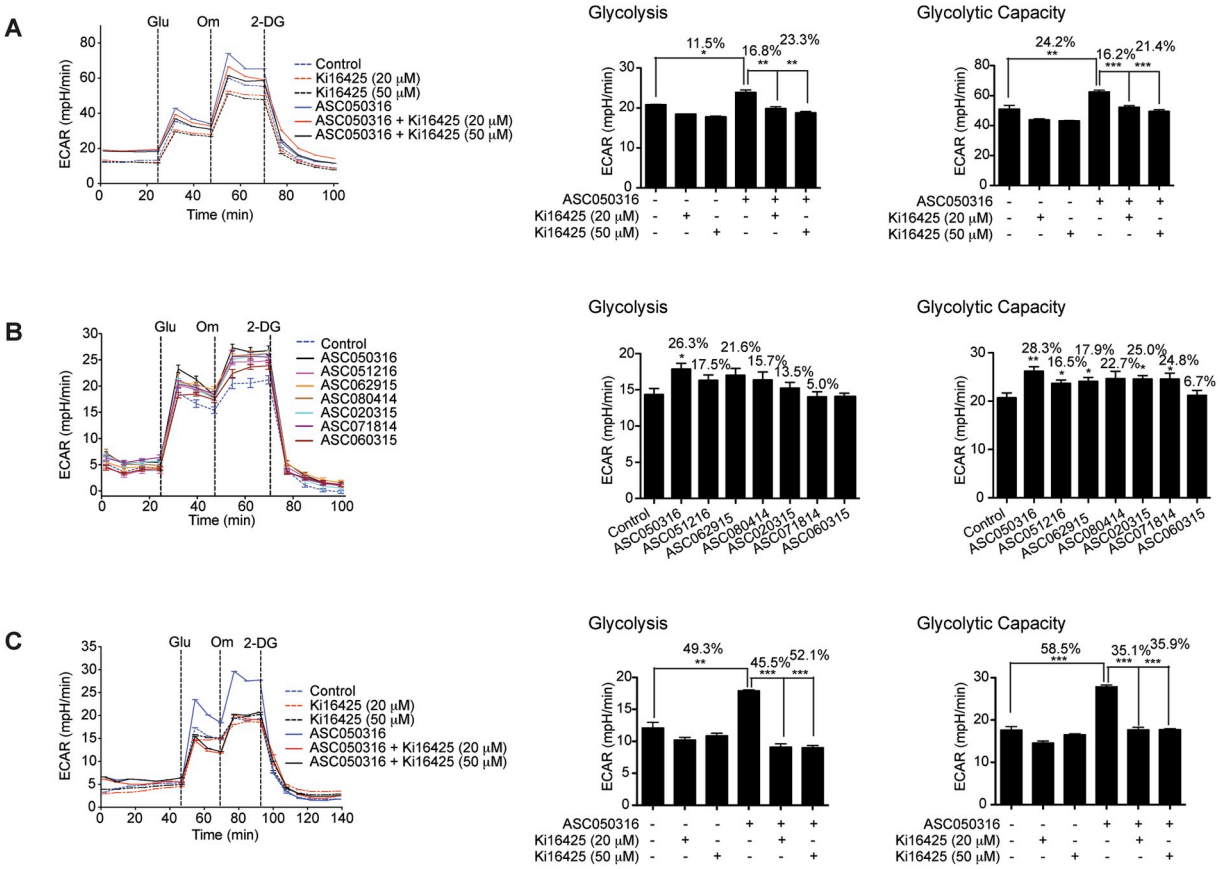

Fig. 5. Ascitic fluid stimulates glycolysis in NFs via LPA-LPAR signaling. A. MRC5 fibroblasts were serum starved overnight and stimulated with 5% ovarian cancer patient-derived ascitic fluid for 6 h. One hour prior to stimulation with ascites fluid, these cells were treated with Ki16425 (20 and 50 μM) or vehicle control. Extracellular flux analysis was carried out using XFe96 analyzer. ECAR profile over time (Left Panel), glycolytic rate and glycolytic capacity (Right Panel) from a representative analysis is presented. Mean and SEM (n = 3 to 11 parallel determinations) is shown. Percentile change over the basal level is denoted over the bars of the chart. **B.** NOF151 cells were stimulated with 5% ascitic fluid samples from 7 different ovarian cancer patients for 6 h. ECAR was analyzed using XFe96 analyzer and glycolysis and glycolytic capacity data from a representative analysis is presented. Percentile stimulation over the control level is denoted over the bars of the chart. Mean and SEM (n = 4 to 7 parallel determinations). **C.** NOF151 cells were pre-treated with Ki16425 (20 and 50 μM) or vehicle control for 1 h prior to stimulation with 5% ascitic fluid ASC050316. ECAR analysis was carried out using XFe96 analyzer and ECAR change over time (Left Panel) glycolysis and glycolytic capacity (Right Panel) is presented. Percentile inhibition over the control level is denoted over the bars of the chart. Mean and SEM (n = 3 to 4 parallel determinations). Statistical significance was determined by Student's *t*-test (*P < 0.05, **P < 0.005, ***P < 0.0005).

3. Results

3.1. Conditioned medium from ovarian cancer cells induce CAF-associated phenotypic changes in MRC5 lung fibroblasts

Cancer cell induced metabolic reprogramming in NFs towards aerobic glycolysis is one of the key features associated with CAF-phenotype [34]. While Soluble factors from cancer cells have been shown to induce glycolysis in CAFs [35], the role of ovarian cancer cell-derived paracrine factors in modulating the CAF-phenotype is largely unknown. To investigate this, conditioned medium collected from ovarian cancer cells OVCAR5 (OVCAR5-CM) was used on MRC5 lung fibroblast model system to monitor the changes in the glycolytic phenotype using an XFe96 analyzer. Briefly, MRC5 cells were treated with OVCAR5-conditioned medium or normal growing (non-conditioned) medium continuously for 5 days. OVCAR5-CM induced glycolysis and glycolytic rate were determined by monitoring the extracellular acidification rate (ECAR) in MRC5 cells. Results from this study showed that OVCAR5-CM was able to induce an increase ECAR in MRC5 fibroblasts compared to the no condition medium control (Fig. 1A). An increase in glycolysis and glycolytic capacity was observed in MRC5 fibroblasts treated with OVCAR5-CM compared to the non-conditioned medium control (Fig. 1A). These findings indicate that the paracrine factors from the ovarian cancer cells can induce a glycolytic phenotype in the neighboring fibroblasts.

Previous studies have also shown that paracrine factors from cancer cells could transform the normal resting fibroblasts to activated cancer associated fibroblasts. Both in vitro studies using conditioned medium from hepatic cancer cells and in vivo xenograft studies in both hepatocellular and melanoma tumors reveal a critical role for cancer cell-derived paracrine factors in the differentiation of NFs to CAFs [35,36] as indicated by the increased expression of FAP, αSMA, growth factor markers like TGFβ1, TGFβ2, PDGF, and bFGF, neo-vascularization markers like VEGF, and chemokine/cytokines like IL6, CXCL12 that are highly associated with transformed CAFs [16–21,37,38]. To determine if paracrine factors from ovarian cancer cells could induce CAF transformation, MRC5 cells were stimulated with conditioned medium from OVCAR5 cells continuously for 10 days. Cells collected at various time points were analyzed for the expression of putative CAF-markers by RT-qPCR analysis. Result from such analysis indicated that OVCAR5-CM induces an increase in the expression of multiple CAF markers such as ACTA2 (αSMA), FAP, TGFβ1, TGFβ2, VEGFA, VEGFB, CXCL12, and IL6 as early as Day 3 (Fig. 1B), thus demonstrating the ability of OVCAR5-CM to induce CAF-associated phenotypic changes in MRC5 fibroblasts.

3.2. LPA induces CAF-phenotypic changes in MRC5 lung fibroblasts

Studies from several laboratories have shown that ovarian cancer

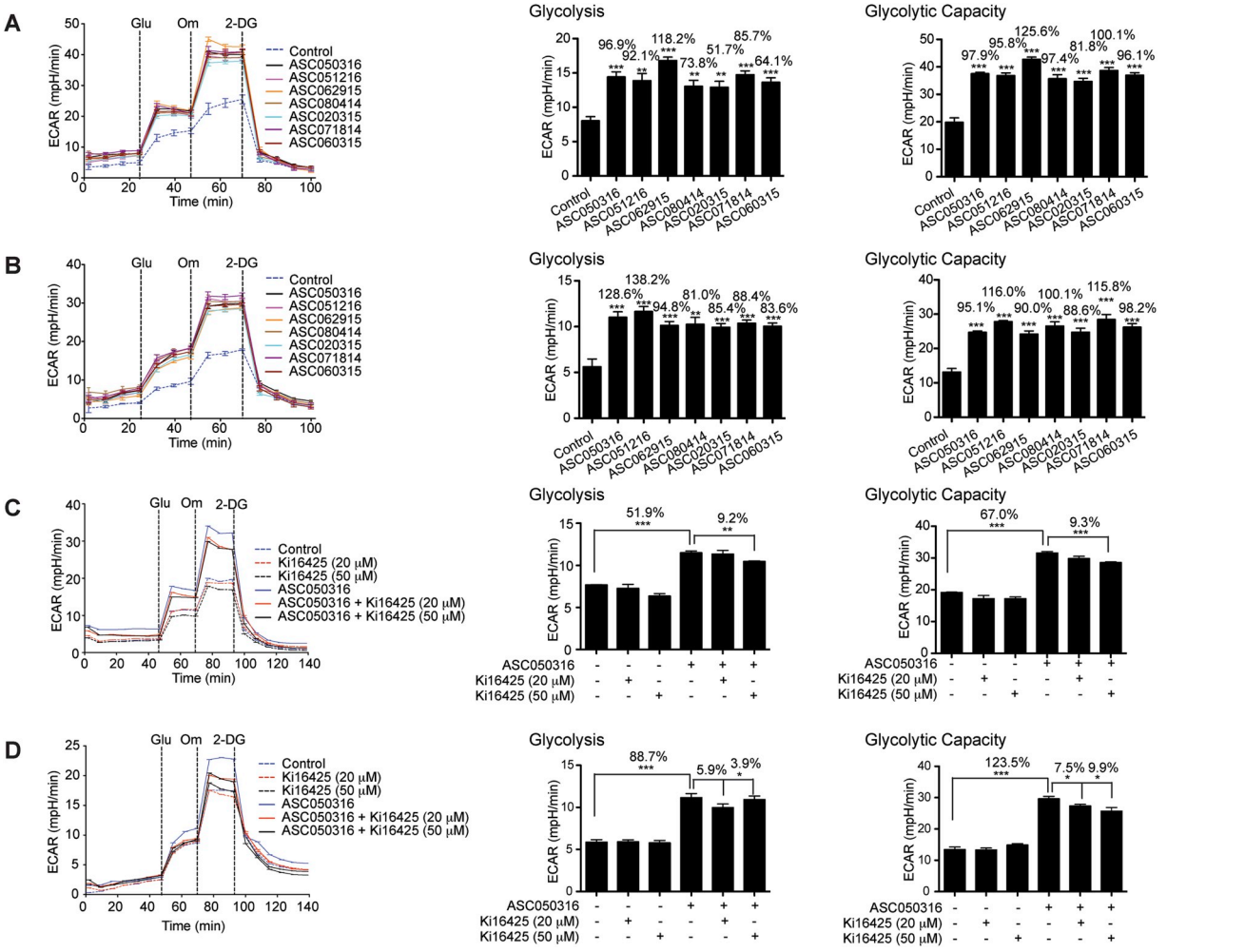

Fig. 6. Ascitic fluid stimulates glycolysis in ovarian CAFs via LPA-LPAR signaling. A & B. Ovarian cancer associated fibroblasts CAF147 and CAF148 were serum starved overnight and stimulated for 6 h with 5% ascitic fluid samples. XFe96 analyzer was used to monitor the changes in glycolysis. ECAR profile over time (*Left Panel*), glycolytic rate and glycolytic capacity (*Right Panel*) from a representative analysis is presented. Mean and SEM (n = 3 to 4 parallel determinations) is shown. Percentile change over the basal level is denoted over the bars of the chart. **C & D.** CAF147 and CAF148 cells were pre-treated with Ki16425 (20 and 50 μM) or vehicle control for 1 h prior to stimulation with 5% ascitic fluid ASC050316. ECAR analysis was carried out using XFe96 analyzer and ECAR change over time (*Left Panel*) glycolysis and glycolytic capacity (*Right Panel*) is presented. Percentile inhibition over the control level is denoted over the bars of the chart. Mean and SEM (n = 3 to 4 parallel determinations). Statistical significance was determined by Student's *t*-test (*P < 0.05, **P < 0.005, ***P < 0.0005).

cells synthesize and secrete LPA into the ascites and the LPA in the ascites can act as a potent mitogenic and motogenic factor in ovarian cancer [39,40]. Our recent studies using high grade serous ovarian carcinoma (HGSOC) cell lines as well as patient-derived ovarian cancer cells have shown that LPA induces a pseudohypoxic oxidative stress and elicits pseudohypoxia-adaptive responses including EMT and metabolic reprogramming towards glycolytic shift in ovarian cancer cells. Therefore, we posited that the LPA secreted by ovarian cancer cells in OCC-CM similarly promotes aerobic glycolysis in fibroblasts. First, we ascertained that LPA is actually present in the CM derived from the ovarian cancer cells. CM from four different HGSOC cell lines and two non-HGSOC cell lines were analyzed for the presence of LPA by ELISA. Results indicated the presence of LPA in CM derived from these cells ranging from 200 nM to 1 μM concentration (Table S2).

Reasoning that the LPA, thus derived, could stimulate glycolysis in the fibroblasts through the activation of membrane-bound LPA-receptors (LPARs), we investigated whether exogenous LPA could induce CAF-associate phenotypic changes in MRC5 fibroblasts. To test, we stimulated MRC5-fibroblasts, with different concentration of LPA for 6 h and glycolysis was measured using XFe96 analyzer. Results from this analysis show that LPA induced an increase in glycolysis and glycolytic capacity in a dose dependent manner (Fig. 2A). We could also demonstrate that the pretreatment of these cells with an increasing concentration of Ki16425, an LPA-receptor antagonist, attenuated LPA-stimulated glycolytic response in these cells (Fig. 2B). These findings further establish the role of LPA and LPARs of the fibroblasts in triggering glycolysis of the fibroblasts. We interrogated further whether LPA could induce the differentiation of MRC5 fibroblasts to a CAF-phenotype, similar to the effect seen with OVCAR5-CM. MRC5 cells were stimulated with 10 μM LPA for 10 days and the cells were analyzed at different time points for the presence of CAF phenotypic markers by RT-qPCR analysis. Results indicate that LPA stimulated the expression of the CAF-markers CXCL12, FAP, TGFβ2, VEGFA, VEGFB, and HIF1α by Day 7 (Fig. 2C). However, LPA did not induce the expression of other CAF markers such as ACTB2, IL6 and TGFβ1 (Fig. 2C). These results suggest that LPA stimulates both functional and molecular CAF-phenotypic changes in MRC5 fibroblasts.

3.3. LPA induces CAF-associated phenotypic changes in normal ovarian fibroblasts (NOFs)

Considering the critical role of LPA in ovarian cancer progression, it is of interest to assess whether LPA could induce such CAF-specific phenotypic changes in fibroblasts derived from ovaries. NOF151, an

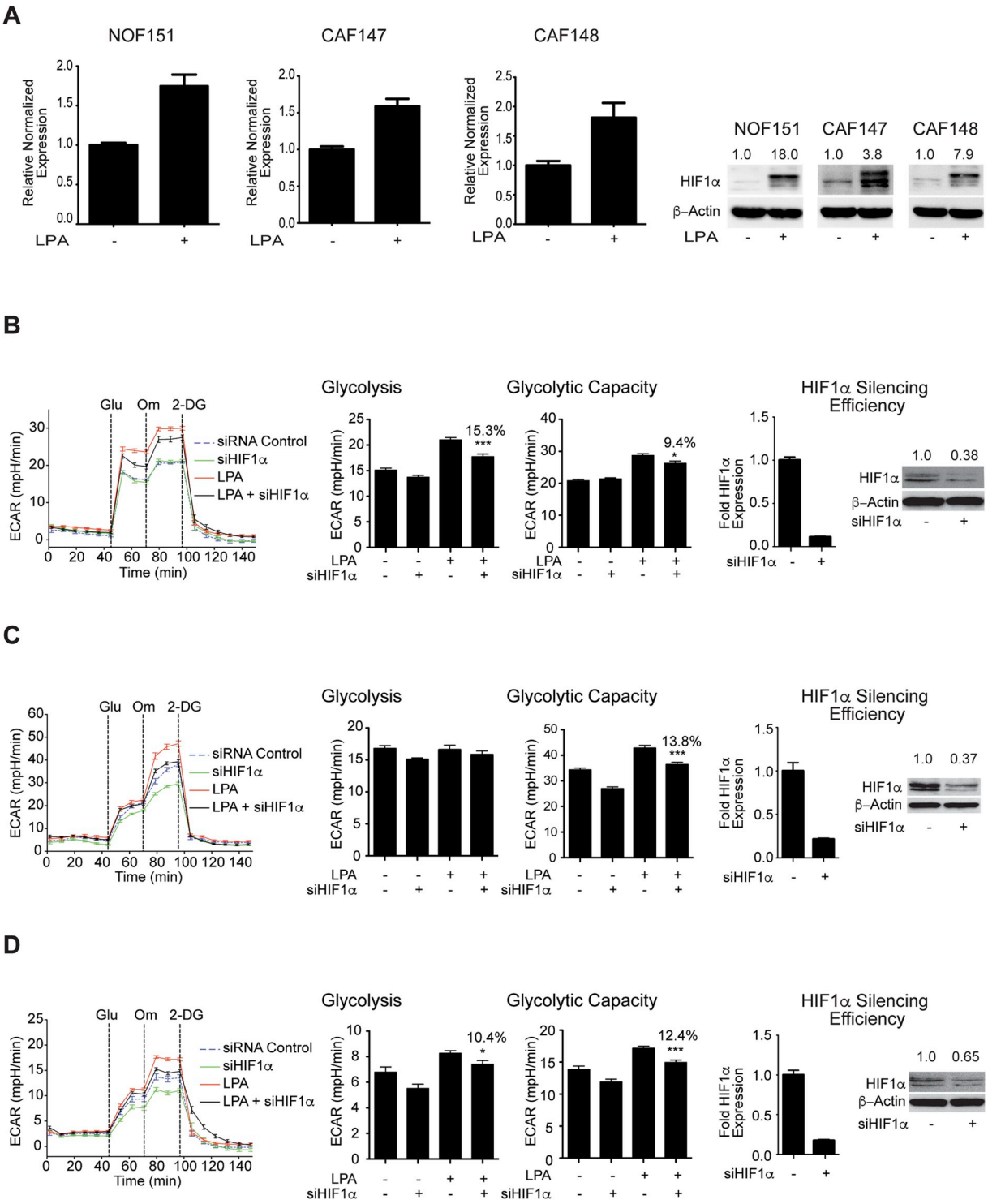

Fig. 7. LPA-induced glycolysis in NOF and ovarian CAFs involves HIF1α. A. NOF151, CAF147 and CAF148 cells were stimulated with 10 μM of LPA for 6 h. Cells were collected and processed for RT-qPCR and immunoblot analyses for HIF1α. HIF1α bands were quantified and the fold increase over the control values is denoted above the HIF1α bands. Results from a typical experiment (n = 3) are presented. **B – D.** NOF151 (B), CAF147 (**C**), and CAF148 (**D**) were transfected with siRNA targeting HIF1α or control non-targeting siRNA for 48 h, following which they were stimulated with 10 μM of LPA for 6 h. ECAR flux over time, glycolysis and glycolytic capacity were plotted. Results (Mean and SEM; n = 6 to 22 parallel determinations) from a representative analysis (n = 3 independent experiments) are presented along with statistical significance, determined by Student *t*-test (*P < 0.05, **P < 0.005, ***P < 0.0005). Percentile decrease over the basal levels of glycolysis is marked above the bars of the histogram. Silencing efficiency was monitored by RT-qPCR and immunoblot analysis for HIF1α. Fold decrease over the control value was quantified and presented over the control levels is presented over the HIF1α bands.

immortalized NOF cell line, was stimulated with increasing concentrations of LPA for 6 h or 48 h and LPA-induced glycolysis was determined using XFe96 analyzer. The results indicated that LPA induced aerobic glycolysis in NOF151 fibroblasts in a dose dependent manner at both the time points (Fig. 3 A & B). LPA-induced stimulation of glycolysis was inhibited by the pretreatment of NOF151 fibroblasts with Ki16425 (Fig. 3C; Fig. S3), indicating the role of LPA-LPAR signaling in this process. Next, we investigated whether LPA could induce molecular

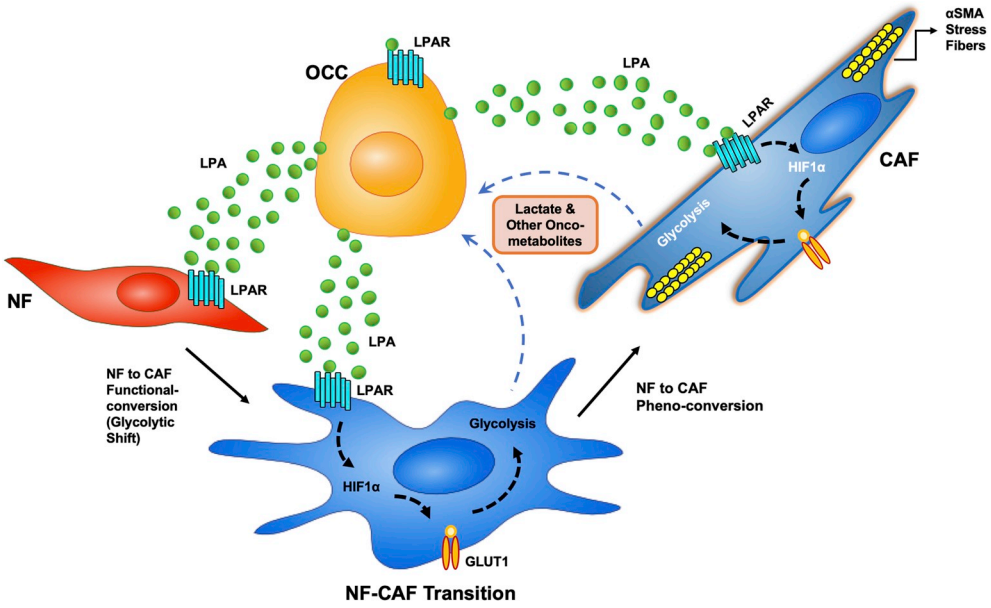

Fig. 8. Schematic representation of LPA-induced transition of normal ovarian fibroblasts to cancer associated fibroblasts. Ovarian cancer cells (OCCs) synthesize and secrete LPA into the ascites of the peritoneal cavity. LPA in the ascites stimulates LPA-receptors (LPAR) in the resident normal fibroblasts (NF) and induces metabolic reprogramming towards aerobic glycolysis *via* HIF1α. This early priming event is followed by the completion of NF to cancer associated fibroblast (CAF) conversion involving LPA-mediated induction of other CAF-specific phenotypic changes such as the expression of α-smooth muscle actin (αSMA). OCC-derived LPA is also involved in the maintenance of the reprogrammed aerobic glycolysis in CAFs *via* HIF1α. Lactate and other oncometabolites generated through this pathway provide metabolic support to OCC, thus contributing to the aggressive growth and progression of ovarian cancer.

phenotypic changes associated with CAFs in NOFs to CAFs. NOF151 cells were stimulated with 10 μM LPA and the expression of CAF-phenotypic markers were monitored over time through immunoblot analysis. Our results show an increase in the expression of CAF-marker αSMA by Day 3 following LPA-stimulation (Fig. 3D). Thus, as in the case of MRC5 fibroblasts (Fig. 2), these results indicate that LPA could stimulate both functional and molecular phenotypic changes represented by glycolytic shift and the expression of CAF-markers in NOFs.

3.4. LPA induces glycolysis in differentiated ovarian CAFs

It has been well documented that CAFs show increased aerobic glycolysis leading to the synthesis of lactate and pyruvate that can be transferred to cancer cells for their increased anabolic need [23,24]. The mechanisms involved in sustaining the increased glycolysis in fully differentiated CAFs are largely unknown. In light of the above observations that LPA-LPAR signaling is involved in inducing glycolysis in NFs, we investigated the role of similar LPA-LPAR signaling loop in sustaining or further enhancing glycolysis in fully trans-differentiated ovarian CAFs. The signaling paradigm involving LPA-LPAR signaling in promoting glycolysis in CAFs was further interrogated by evaluating the ability of LPA to induce aerobic glycolysis in ovarian CAFs. To analyze, previously established CAF cell lines, namely CAF147 and CAF148, were stimulated with increasing concentrations of LPA and glycolysis in response to LPA was monitored at the end of 6 h. Results from this analysis demonstrated the ability of LPA to promote an increase in glycolysis and the glycolytic capacity in both CAF147 and CAF148 cells (Fig. 4A and B). Furthermore, this increase in ECAR was abrogated by the pretreatment of the CAFs with Ki16425, indicating that LPA-LPAR signaling pathways is involved in sustaining and/or further enhancing glycolysis in ovarian CAFs (Fig. 4 Cand D).

3.5. Ascitic fluid stimulates glycolysis in NFs and ovarian CAFs via LPA-LPAR signaling

Our findings that LPA induces CAF-phenotype in NFs become highly significant in the context of ovarian cancer in which the cancer tissues are continuously bathed in ascitic fluid that contains high concentrations of LPA [41–44]. Therefore, we investigated whether ascitic fluid derived from ovarian cancer patients can induce glycolytic shift in ovarian fibroblasts and if so, whether it is mediated by LPA. First, we determined the concentration of LPA in the ascitic fluid obtained from seven ovarian cancer patients. ELISA analysis of the ascites samples indicated the presence LPA in μM concentrations ranging from 23 μM to 150 μM (Table S3) in agreement with the previous findings [41–44]. Next, we analyzed the ability of ascites to stimulate glycolytic shift in MRC5 and NOF151 fibroblasts. MRC5 and NOF151 cells were treated with 5% of the individual ascitic fluid samples for 6 h and at the end of 6 h, the cells were analyzed for glycolytic shift. Results indicated that the tested ascites samples stimulated the glycolytic flux in both MRC5 and NOF151 cells (Fig. 5 & S1). In fact, all of the tested ascites samples stimulated such increased glycolysis in NOF151 cell lines (Fig. S1, Fig. 5B). More importantly, pre-treatment of the MRC5 (Fig. 5A) or NOF151 (Fig. 5C) cells with Ki16425 attenuated ascites-stimulated glycolysis. Taken together, these results point to the role of ascites-contained LPA, presumably secreted by the ovarian cancer cells, in triggering aerobic glycolysis, thus metabolic CAF-phenotype in NFs. Next, we explored the possibility that a similar LPA-LPAR signaling pathways is involved in inducing and possibly maintaining the glycolytic phenotype in fully differentiated ovarian CAFs. To test, ovarian CAF cell lines, CAF147 and CAF 148 were stimulated with ascites samples for 6 hrs in the presence and absence of Ki16425 following which the glycolytic flux was monitored. Results from this analysis indicated that the ascites fluid could stimulate an increase in ECAR even in fully differentiated ovarian CAFs (Fig. 6 A & B) and that this increase was inhibited by pre-treatment with Ki16425 (Fig. 6C and D).

3.6. LPA-induced glycolysis in NOF and ovarian CAFs involve HIF1α

Our recent studies have shown that LPA induces pseudohypoxic oxidative stress and elicits pseudohypoxia-adaptive responses including EMT and metabolic reprogramming in ovarian cancer cells [28]. We have also shown that the adaptive response involves the LPA-LPAR mediated increase in the expression and/or stabilization of HIF1α [28]. Therefore, we focused on defining whether LPA-LPAR-HIF1α signaling paradigm is involved in the observed stimulation of glycolysis in ovarian NOFs and CAFs. To validate such a paradigm, first we tested whether LPA could stimulate the expression of HIF1α in ovarian NOFs and CAFs. NOF151 as well as CAF147 and CAF148 were stimulated with LPA for 6 h. Expression of HIF1α was monitored by RT-qPCR and immunoblot analyses. Results from this study show that LPA stimulates the expression of HIF1α in both the NOFs and CAFs (Fig. 7A). Next, we analyzed whether LPA-induced increase in glycolysis is mediated

through HIF1α. Expression of HIF1α was silenced using siRNA to HIF1α in NOF151, CAF147 and CAF148 fibroblasts. Thereafter, the cells were stimulated with LPA for 6 h and the glycolytic rates were monitored. Results indicated that the silencing of HIF1α abrogated glycolysis in the NOF151 (Fig. 7B) as well as CAF147 and CAF148 (Fig. 7C and D) suggesting the dominant role of HIF1α in LPA-LPAR signaling induced glycolysis, a major functional phenotype of ovarian CAFs. These results highlight the pivotal role of HIF1α in LPA-LPAR mediated paracrine signaling in triggering and presumably maintaining a functional CAF-phenotype in resident fibroblasts in the TME (see Fig. 8).

4. Discussion

TME plays a major role in the pathogenesis and progression of several cancers including ovarian cancers [45]. Cancer-associated fibroblasts comprise one of the most important cellular components in the TME [2,46,47]. With the growing evidence that CAFs promote progression and metastasis of many cancers, defining the mechanism underlying the differentiation of NFs to a CAFs has become critically important to develop novel therapy. Although diverse cancer-derived growth factors and oncometabolites have been shown to be associated with the trans-differentiation of NFs to CAFs, precise roles of these molecules are not fully understood [48]. Hypoxia has been known to induce the trans-differentiation of NFs to CAFs [49]. Here we show that LPA induces such trans-differentiation even under normoxic condition. Our recent studies have shown that LPA induces pseudohypoxia-induced oxidative stress in ovarian cancer cells with the resultant expression of HIF1α via the signaling nexus involving Gαi2, Rac1, NOX2, and the generation of ROS [28]. This in turn elicits an adaptive HIF1α-dependent pseudohypoxia adaptive response that includes the increased expression of GLUT1 and HK2 with the subsequent triggering of glycolytic shift in ovarian cancer cells. Here we show that an analogous LPA-LPAR -mediated pseudohypoxia with an increased expression of HIF1α and HIF1α mediated pseudohypoxia-adaptive mechanisms are involved in transitioning NOFs to CAF-phenotype. However, a notable difference is that the LPA-LPAR induced pseudohypoxia in ovarian cancer cells involves an autocrine signaling loop whereas it involves a paracrine signaling mechanism involving LPA secreted by the ovarian cancer cells and the membrane-bound LPARs in adjacent fibroblasts. TME in ovarian cancer is a highly complex niche with the presence of several growth factors, chemokines, cytokines and angiogenic factors [50–52]. Several of these factors such as IL6, TGFβ, TGF-β2, PDGF, VEGF, and CXCL12 have been identified to induce NOFs to CAFs [17,21,35,38]. Interestingly, LPA is known to stimulate the synthesis and secretion of several of these cytokines and chemokines in ovarian cancer cells [39,53]. Thus, it is possible that ovarian cancer cell-derived LPA triggers the initial signaling events in the resident ovarian NOFs in the TME to promote CAF-phenotypic changes.

It is of interest to note here that LPA has been shown to stimulate the expression of αSMA-expression, thus CAF/myofibroblast phenotype, in hepatocellular carcinoma associated peritumoral fibroblasts [36] and human adipose tissue derived mesenchymal stem cells (hASCs) by 4 days [54,55]. Our results with NFs also show that LPA-induced αSMA expression can be seen in the fibroblasts by day 3, thus suggesting a possible universal LPA-mediated mechanism underlying the transition of mesenchymal stem cells and NFs to CAF-phenotype. Studies with hASCs have also indicated that LPA induced expression of αSMA involves both RhoA and TGFβ1 [54,55]. Here we show that these events are preceded by a glycolytic shift in normal fibroblasts that is triggered by LPA.

A three-step model has been proposed for the phenotypic differentiation of NOFs to CAFs [8]. The steps envisaged by this model encompasses 1) tumor cell mediated NOF-recruitment; 2) induction of CAF-phenotype; and 3) maintenance of CAF-phonotype. However, based on the wide heterogeneity in terms of the putative CAF-markers or signatures, it has also been opined that CAFs represent a “dynamic state” rather than specific cell type [1]. While both these scenarios are not mutually exclusive, the acquired CAF-phenotype by fibroblasts in the TME plays a critical role in cancer progression and metastasis. Our studies presented here suggest that the induction of NOFs to CAF-phenotype involves at least two steps. The first step involves the priming of the NOFs through the stimulation of glycolysis, a key functional signature, indicative of CAF-phenotype. The second step involves the maturation of CAF-phenotype with the expression of the full complement of CAF-markers. In light of the present findings that LPA induced expression of HIF1α along with the HIF1α-mediated glycolytic shift is an early response and HIF1α induces the expression of RhoA in diverse cell types [56,57] and TGFβ1/Smad signaling, especially in fibroblasts [58], it is likely that the LPA-LPAR-HIF1α initiate the CAF-phenotypic programming in ovarian fibroblasts in the TME. Further studies should define the finer role of these signaling components stimulated by LPA in NOF to CAF-transition in the ovarian TME. The observation that the glycolytic shift in NOFs is inhibited by the LPAR-antagonists Ki16425 support the view that it is the LPA released by ovarian cancer cells (either in the CM in vitro or in the ascites in vivo) that initiates the metabolic changes that determine the NOFs to CAFs transition as well as the maintenance of the glycolytic phenotype in matured CAFs (Fig. 8). Furthermore, the findings that LPAR-antagonist can abrogate ascites induced metabolic reprogramming in NOFs as well as CAFs indicates that LPA-LPAR-HIF1α pathway can be targeted to inhibit the functional transformation of CAFs. From a translational point of view, our observations that LPA induces pseudohypoxia and the subsequent adaptive metabolic reprogramming in both the cancer cell- and peritumoral fibroblast-compartments, qualify LPA-LPAR-HIF1α signaling nexus as a potential candidate for the development of multi-target drug development strategy in ovarian cancer.

Conflicts of interest statement

The authors declare that there is no conflict of interest.

Acknowledgment

This research was supported by National Institutes of Health grant GM103639 (to D.N. Dhanasekaran & J.H. Ha); National Research Foundation of Korea BK Program grant 2009-0093820, the BK21 Plus Program grant 5256-20140100 (Y.S. Song); and Grants from Stephenson Cancer Center, OUHSC, Oklahoma City, OK; Mary K. Chapman Foundation Grant Award for Stephenson Cancer Center-MD Anderson Collaborative Research (D.N. Dhanasekaran, K.M. Moxley, J. Liu, and A.K. Sood). Technical assistance by Dr. Chiara Vidoni and Ms. Alessandra Ferraresi, Università del Piemonte Orientale, is gratefully acknowledged. Tissue acquisition and pathology services, provided by the Biorepository Core and the Biospecimen Pathology Core of the Stephenson Cancer Center, were supported by the National Institute of General Medical Sciences Grant P20 GM103639 and the National Cancer Institute Grant P30CA225520 of the National Institutes of Health.

Appendix A. Supplementary data

Supplementary data to this article can be found online at https://doi.org/10.1016/j.canlet.2018.11.023.

References

[1] S. Madar, I. Goldstein, V. Rotter, 'Cancer associated fibroblasts'–more than meets the eye, Trends Mol. Med. 19 (2013) 447–453.
[2] R. Kalluri, The biology and function of fibroblasts in cancer, Nat. Rev. Canc. 16 (2016) 582–598.
[3] J.S.K. Chan, M.K. Sng, Z.Q. Teo, H.C. Chong, J.S. Twang, N.S. Tan, Targeting nuclear receptors in cancer-associated fibroblasts as concurrent therapy to inhibit development of chemoresistant tumors, Oncogene 37 (2018) 160–173.

[4] V.S. LeBleu, R. Kalluri, A peek into cancer-associated fibroblasts: origins, functions and translational impact, Dis. Model Mech. 11 (2018).
[5] S. Ma, S. Pradeep, W. Hu, D. Zhang, R. Coleman, A. Sood, The role of tumor microenvironment in resistance to anti-angiogenic therapy, F1000Res 7 (2018) 326.
[6] Y. Han, U. Cho, S. Kim, I.S. Park, J.H. Cho, D.N. Dhanasekaran, Y.S. Song, Tumour microenvironment on mitochondrial dynamics and chemoresistance in cancer, Free Radic. Res. (2018) 1–17.
[7] L. Tao, G. Huang, H. Song, Y. Chen, L. Chen, Cancer associated fibroblasts: an essential role in the tumor microenvironment, Oncol Lett. 14 (2017) 2611–2620.
[8] P. Heneberg, Paracrine tumor signaling induces transdifferentiation of surrounding fibroblasts, Crit. Rev. Oncol. Hematol. 97 (2016) 303–311.
[9] A. Arina, C. Idel, E.M. Hyjek, M.L. Alegre, Y. Wang, V.P. Bindokas, R.R. Weichselbaum, H. Schreiber, Tumor-associated fibroblasts predominantly come from local and not circulating precursors, Proc. Natl. Acad. Sci. U. S. A. 113 (2016) 7551–7556.
[10] P. Garin-Chesa, L.J. Old, W.J. Rettig, Cell surface glycoprotein of reactive stromal fibroblasts as a potential antibody target in human epithelial cancers, Proc. Natl. Acad. Sci. U. S. A. 87 (1990) 7235–7239.
[11] M.M. Mueller, N.E. Fusenig, Friends or foes - bipolar effects of the tumour stroma in cancer, Nat. Rev. Canc. 4 (2004) 839–849.
[12] N. Nair, A.S. Calle, M.H. Zahra, M. Prieto-Vila, A.K.K. Oo, L. Hurley, A. Vaidyanath, A. Seno, J. Masuda, Y. Iwasaki, H. Tanaka, T. Kasai, M. Seno, A cancer stem cell model as the point of origin of cancer-associated fibroblasts in tumor microenvironment, Sci. Rep. 7 (2017) 6838.
[13] P.A. Kenny, G.Y. Lee, M.J. Bissell, Targeting the tumor microenvironment, Front. Biosci. 12 (2007) 3468–3474.
[14] M. Li, M. Li, T. Yin, H. Shi, Y. Wen, B. Zhang, M. Chen, G. Xu, K. Ren, Y. Wei, Targeting of cancerassociated fibroblasts enhances the efficacy of cancer chemotherapy by regulating the tumor microenvironment, Mol. Med. Rep. 13 (2016) 2476–2484.
[15] D.H. Suh, H.S. Kim, B. Kim, Y.S. Song, Metabolic orchestration between cancer cells and tumor microenvironment as a co-evolutionary source of chemoresistance in ovarian cancer: a therapeutic implication, Biochem. Pharmacol. 92 (2014) 43–54.
[16] Y. Crawford, I. Kasman, L. Yu, C. Zhong, X. Wu, Z. Modrusan, J. Kaminker, N. Ferrara, PDGF-C mediates the angiogenic and tumorigenic properties of fibroblasts associated with tumors refractory to anti-VEGF treatment, Cancer Cell 15 (2009) 21–34.
[17] J. Dong, J. Grunstein, M. Tejada, F. Peale, G. Frantz, W.C. Liang, W. Bai, L. Yu, J. Kowalski, X. Liang, G. Fuh, H.P. Gerber, N. Ferrara, VEGF-null cells require PDGFR alpha signaling-mediated stromal fibroblast recruitment for tumorigenesis, EMBO J. 23 (2004) 2800–2810.
[18] J. Fang, L. Yan, Y. Shing, M.A. Moses, HIF-1alpha-mediated up-regulation of vascular endothelial growth factor, independent of basic fibroblast growth factor, is important in the switch to the angiogenic phenotype during early tumorigenesis, Cancer Res. 61 (2001) 5731–5735.
[19] M. Allinen, R. Beroukhim, L. Cai, C. Brennan, J. Lahti-Domenici, H. Huang, D. Porter, M. Hu, L. Chin, A. Richardson, S. Schnitt, W.R. Sellers, K. Polyak, Molecular characterization of the tumor microenvironment in breast cancer, Cancer Cell 6 (2004) 17–32.
[20] T. Silzle, M. Kreutz, M.A. Dobler, G. Brockhoff, R. Knuechel, L.A. Kunz-Schughart, Tumor-associated fibroblasts recruit blood monocytes into tumor tissue, Eur. J. Immunol. 33 (2003) 1311–1320.
[21] A. Orimo, P.B. Gupta, D.C. Sgroi, F. Arenzana-Seisdedos, T. Delaunay, R. Naeem, V.J. Carey, A.L. Richardson, R.A. Weinberg, Stromal fibroblasts present in invasive human breast carcinomas promote tumor growth and angiogenesis through elevated SDF-1/CXCL12 secretion, Cell 121 (2005) 335–348.
[22] D. Kumar, J. New, V. Vishwakarma, R. Joshi, J. Enders, F. Lin, S. Dasari, W.R. Gutierrez, G. Leef, S. Ponnurangam, H. Chavan, L. Ganaden, M.M. Thornton, H. Dai, O. Tawfik, J. Straub, Y. Shnayder, K. Kakarala, T.T. Tsue, D.A. Girod, B. Van Houten, S. Anant, P. Krishnamurthy, S.M. Thomas, Cancer-associated fibroblasts drive glycolysis in a targetable signaling loop implicated in head and neck squamous cell carcinoma progression, Cancer Res. 78 (2018) 3769–3782.
[23] S. Pavlides, D. Whitaker-Menezes, R. Castello-Cros, N. Flomenberg, A.K. Witkiewicz, P.G. Frank, M.C. Casimiro, C. Wang, P. Fortina, S. Addya, R.G. Pestell, U.E. Martinez-Outschoorn, F. Sotgia, M.P. Lisanti, The reverse Warburg effect: aerobic glycolysis in cancer associated fibroblasts and the tumor stroma, Cell Cycle 8 (2009) 3984–4001.
[24] F. Sotgia, D. Whitaker-Menezes, U.E. Martinez-Outschoorn, N. Flomenberg, R.C. Birbe, A.K. Witkiewicz, A. Howell, N.J. Philp, R.G. Pestell, M.P. Lisanti, Mitochondrial metabolism in cancer metastasis: visualizing tumor cell mitochondria and the "reverse Warburg effect" in positive lymph node tissue, Cell Cycle 11 (2012) 1445–1454.
[25] Y. Fu, S. Liu, S. Yin, W. Niu, W. Xiong, M. Tan, G. Li, M. Zhou, The reverse Warburg effect is likely to be an Achilles' heel of cancer that can be exploited for cancer therapy, Oncotarget 8 (2017) 57813–57825.
[26] F. Xing, J. Saidou, K. Watabe, Cancer associated fibroblasts (CAFs) in tumor microenvironment, Front Biosci (Landmark Ed) 15 (2010) 166–179.
[27] R.L. Siegel, K.D. Miller, A. Jemal, Cancer statistics, CA A Cancer J. Clin. 67 (2017) 7–30 2017.
[28] J.H. Ha, R. Radhakrishnan, M. Jayaraman, M. Yan, J.D. Ward, K.M. Fung, K. Moxley, A.K. Sood, C. Isidoro, P. Mukherjee, Y.S. Song, D.N. Dhanasekaran, LPA induces metabolic reprogramming in ovarian cancer via a pseudohypoxic response, Cancer Res. 78 (2018) 1923–1934.
[29] A. Toullec, D. Gerald, G. Despouy, B. Bourachot, M. Cardon, S. Lefort, M. Richardson, G. Rigaill, M.C. Parrini, C. Lucchesi, D. Bellanger, M.H. Stern, T. Dubois, X. Sastre-Garau, O. Delattre, A. Vincent-Salomon, F. Mechta-Grigoriou, Oxidative stress promotes myofibroblast differentiation and tumour spreading, EMBO Mol. Med. 2 (2010) 211–230.
[30] D. Whitaker-Menezes, U.E. Martinez-Outschoorn, Z. Lin, A. Ertel, N. Flomenberg, A.K. Witkiewicz, R.C. Birbe, A. Howell, S. Pavlides, R. Gandara, R.G. Pestell, F. Sotgia, N.J. Philp, M.P. Lisanti, Evidence for a stromal-epithelial "lactate shuttle" in human tumors: MCT4 is a marker of oxidative stress in cancer-associated fibroblasts, Cell Cycle 10 (2011) 1772–1783.
[31] I.G. Schauer, J. Zhang, Z. Xing, X. Guo, I. Mercado-Uribe, A.K. Sood, P. Huang, J. Liu, Interleukin-1beta promotes ovarian tumorigenesis through a p53/NF-kappaB-mediated inflammatory response in stromal fibroblasts, Neoplasia 15 (2013) 409–420.
[32] R.N. Kumar, J.H. Ha, R. Radhakrishnan, D.N. Dhanasekaran, Transactivation of platelet-derived growth factor receptor alpha by the GTPase-deficient activated mutant of Galpha12, Mol. Cell Biol. 26 (2006) 50–62.
[33] H.W. Hirte, D.A. Clark, J. Mazurka, G. O'Connell, J. Rusthoven, A rapid and simple method for the purification of tumor cells from ascitic fluid of ovarian carcinoma, Gynecol. Oncol. 44 (1992) 223–226.
[34] U. Martinez-Outschoorn, F. Sotgia, M.P. Lisanti, Tumor microenvironment and metabolic synergy in breast cancers: critical importance of mitochondrial fuels and function, Semin. Oncol. 41 (2014) 195–216.
[35] D. Zhang, Y. Wang, Z. Shi, J. Liu, P. Sun, X. Hou, J. Zhang, S. Zhao, B.P. Zhou, J. Mi, Metabolic reprogramming of cancer-associated fibroblasts by IDH3alpha down-regulation, Cell Rep. 10 (2015) 1335–1348.
[36] A. Mazzocca, F. Dituri, L. Lupo, M. Quaranta, S. Antonaci, G. Giannelli, Tumor-secreted lysophostatidic acid accelerates hepatocellular carcinoma progression by promoting differentiation of peritumoral fibroblasts in myofibroblasts, Hepatology 54 (2011) 920–930.
[37] H. Sugimoto, T.M. Mundel, M.W. Kieran, R. Kalluri, Identification of fibroblast heterogeneity in the tumor microenvironment, Cancer Biol. Ther. 5 (2006) 1640–1646.
[38] L. Hlatky, C. Tsionou, P. Hahnfeldt, C.N. Coleman, Mammary fibroblasts may influence breast tumor angiogenesis via hypoxia-induced vascular endothelial growth factor up-regulation and protein expression, Cancer Res. 54 (1994) 6083–6086.
[39] X. Fang, M. Schummer, M. Mao, S. Yu, F.H. Tabassam, R. Swaby, Y. Hasegawa, J.L. Tanyi, R. LaPushin, A. Eder, R. Jaffe, J. Erickson, G.B. Mills, Lysophosphatidic acid is a bioactive mediator in ovarian cancer, Biochim. Biophys. Acta 1582 (2002) 257–264.
[40] T.L. Pua, F.Q. Wang, D.A. Fishman, Roles of LPA in ovarian cancer development and progression, Future Oncol. 5 (2009) 1659–1673.
[41] G.B. Mills, C. May, M. McGill, C.M. Roifman, A. Mellors, A putative new growth factor in ascitic fluid from ovarian cancer patients: identification, characterization, and mechanism of action, Cancer Res. 48 (1988) 1066–1071.
[42] Y. Xu, D.C. Gaudette, J.D. Boynton, A. Frankel, X.J. Fang, A. Sharma, J. Hurteau, G. Casey, A. Goodbody, A. Mellors, et al., Characterization of an ovarian cancer activating factor in ascites from ovarian cancer patients, Clin. Canc. Res. 1 (1995) 1223–1232.
[43] Y. Xu, Z. Shen, D.W. Wiper, M. Wu, R.E. Morton, P. Elson, A.W. Kennedy, J. Belinson, M. Markman, G. Casey, Lysophosphatidic acid as a potential biomarker for ovarian and other gynecologic cancers, J. Am. Med. Assoc. 280 (1998) 719–723.
[44] D.L. Baker, P. Morrison, B. Miller, C.A. Riely, B. Tolley, A.M. Westermann, J.M. Bonfrer, E. Bais, W.H. Moolenaar, G. Tigyi, Plasma lysophosphatidic acid concentration and ovarian cancer, J. Am. Med. Assoc. 287 (2002) 3081–3082.
[45] A. Ghoneum, H. Afify, Z. Salih, M. Kelly, N. Said, Role of tumor microenvironment in ovarian cancer pathobiology, Oncotarget 9 (2018) 22832–22849.
[46] M. Allen, J. Louise Jones, Jekyll and Hyde: the role of the microenvironment on the progression of cancer, J. Pathol. 223 (2011) 162–176.
[47] S. Thongchot, A. Ferraresi, C. Vidoni, W. Loilome, P. Yongvanit, N. Namwat, C. Isidoro, Resveratrol interrupts the pro-invasive communication between cancer associated fibroblasts and cholangiocarcinoma cells, Cancer Lett. 430 (2018) 160–171.
[48] C.A. Lyssiotis, A.C. Kimmelman, Metabolic interactions in the tumor microenvironment, Trends Cell Biol. 27 (2017) 863–875.
[49] V. Petrova, M. Annicchiarico-Petruzzelli, G. Melino, I. Amelio, The hypoxic tumour microenvironment, Oncogenesis 7 (2018) 10.
[50] N. Ahmed, K.L. Stenvers, Getting to know ovarian cancer ascites: opportunities for targeted therapy-based translational research, Front. Oncol. 3 (2013) 256.
[51] T. Worzfeld, E. Pogge von Strandmann, M. Huber, T. Adhikary, U. Wagner, S. Reinartz, R. Muller, The unique molecular and cellular microenvironment of ovarian cancer, Front. Oncol. 7 (2017) 24.
[52] C. Thuwajit, A. Ferraresi, R. Titone, P. Thuwajit, C. Isidoro, The metabolic cross-talk between epithelial cancer cells and stromal fibroblasts in ovarian cancer progression: autophagy plays a role, Med. Res. Rev. 38 (2018) 1235–1254.
[53] X. Fang, S. Yu, R.C. Bast, S. Liu, H.J. Xu, S.X. Hu, R. LaPushin, F.X. Claret, B.B. Aggarwal, Y. Lu, G.B. Mills, Mechanisms for lysophosphatidic acid-induced cytokine production in ovarian cancer cells, J. Biol. Chem. 279 (2004) 9653–9661.
[54] E.S. Jeon, H.J. Moon, M.J. Lee, H.Y. Song, Y.M. Kim, M. Cho, D.S. Suh, M.S. Yoon, C.L. Chang, J.S. Jung, J.H. Kim, Cancer-derived lysophosphatidic acid stimulates differentiation of human mesenchymal stem cells to myofibroblast-like cells, Stem Cell. 26 (2008) 789–797.
[55] E.S. Jeon, S.C. Heo, I.H. Lee, Y.J. Choi, J.H. Park, K.U. Choi, D.Y. Park, D.S. Suh, M.S. Yoon, J.H. Kim, Ovarian cancer-derived lysophosphatidic acid stimulates secretion of VEGF and stromal cell-derived factor-1 alpha from human mesenchymal stem cells, Exp. Mol. Med. 42 (2010) 280–293.
[56] D.M. Gilkes, L. Xiang, S.J. Lee, P. Chaturvedi, M.E. Hubbi, D. Wirtz, G.L. Semenza, Hypoxia-inducible factors mediate coordinated RhoA-ROCK1 expression and signaling in breast cancer cells, Proc. Natl. Acad. Sci. U. S. A. 111 (2014) E384–E393.
[57] A.E. Greijer, P. van der Groep, D. Kemming, A. Shvarts, G.L. Semenza, G.A. Meijer, M.A. van de Wiel, J.A. Belien, P.J. van Diest, E. van der Wall, Up-regulation of gene expression by hypoxia is mediated predominantly by hypoxia-inducible factor 1 (HIF-1), J. Pathol. 206 (2005) 291–304.
[58] X. Mingyuan, P. Qianqian, X. Shengquan, Y. Chenyi, L. Rui, S. Yichen, X. Jinghong, Hypoxia-inducible factor-1alpha activates transforming growth factor-beta1/Smad signaling and increases collagen deposition in dermal fibroblasts, Oncotarget 9 (2018) 3188–3197.